Aldona Ząber-Kucharska[1], Przemysław Olbratowski[2–4], Józef Ginter[5], Natalia Gołuchowska[1], Bolesław Kalicki[1,5], Agata Tomaszewska[1,5]

Received: 22.03.2026
Accepted: 19.05.2026
Published: 09.07.2026

A machine-learning model for quantitative assessment of maxillary sinus volume and involvement in children based on computed tomography

Algorytm uczenia maszynowego do automatycznej oceny objętości i stopnia zajęcia zatok szczękowych u dzieci na podstawie badań tomografii komputerowej

[1] Department of Paediatrics, Paediatric Nephrology and Allergology, Military Institute of Medicine – National Research Institute, Warsaw, Poland
[2] Faculty of Physics, University of Warsaw, Warsaw, Poland
[3] Biological and Chemical Research Centre, University of Warsaw, Warsaw, Poland
[4] WIT Academy, Warsaw, Poland
[5] Faculty of Medicine, University of Warsaw, Warsaw, Poland
Correspondence: Aldona Ząber-Kucharska, Department of Paediatrics, Paediatric Nephrology and Allergology, Military Institute of Medicine – National Research Institute, Szaserów 128, 04-141 Warsaw, Poland, e-mail: aldonazaber@gmail.com

https://doi.org/10.15557/PiMR.2026.0012

ORCID iDs
1. Aldona Ząber-Kucharska https://orcid.org/0009-0004-3577-3203
2. Józef Ginter https://orcid.org/0000-0001-7581-5296
3. Natalia Gołuchowska https://orcid.org/0000-0002-1928-175X
4. Bolesław Kalicki https://orcid.org/0000-0003-1606-5100
5. Agata Tomaszewska https://orcid.org/0000-0003-3255-7623

Abstract

Introduction: Chronic rhinosinusitis in children represents a significant clinical challenge. Imaging-based diagnosis relies primarily on descriptive assessment of computed tomography scans and simplified scoring systems that do not account for the actual volume of inflammatory lesions. A more quantitative analysis of sinus involvement could improve diagnostic accuracy and reduce interobserver variability. **Objective:** The aim of this study was to develop a machine learning algorithm for the automated quantitative assessment of maxillary sinus volume and inflammatory involvement in children based on computed tomography scans. **Materials and methods:** The study includes 92 computed tomography scans of the paranasal sinuses obtained from paediatric patients, with the maxillary sinuses manually annotated by human experts. A three-dimensional convolutional neural network was developed for sinus segmentation. Based on the segmentation results, sinus volume and the percentage of sinus involvement by inflammatory changes were calculated. **Results:** The algorithm demonstrates high segmentation performance, achieving mean sensitivity, precision, and Dice coefficient values of nearly 90%. The root-mean-square error for estimation of sinus volume and inflammatory involvement is 0.4 cm^3 and 1.3 percentage points, respectively. **Conclusions:** The proposed approach enables rapid and precise assessment of maxillary sinus volume and the extent of inflammatory involvement in paediatric computed tomography examinations. It may serve as a valuable tool supporting clinical decision-making in the diagnosis and longitudinal monitoring of chronic rhinosinusitis in children.

Keywords: paediatric chronic rhinosinusitis, maxillary sinus, volumetric analysis, computed tomography, medical image segmentation, convolutional neural network, deep learning, artificial intelligence

Streszczenie

Wprowadzenie: Przewlekłe zapalenie zatok przynosowych u dzieci stanowi istotny problem kliniczny. Diagnostyka obrazowa opiera się przede wszystkim na opisowej ocenie badań tomografii komputerowej i uproszczonych skalach punktowych, które nie uwzględniają rzeczywistej objętości zmian zapalnych. Bardziej ilościowa analiza mogłaby poprawić dokładność diagnozy i zmniejszyć zmienność międzyobserwacyjną. **Cel:** Celem niniejszej pracy jest stworzenie algorytmu uczenia maszynowego do automatycznej ilościowej oceny objętości i zajęcia zatok szczękowych u dzieci na podstawie badań tomografii komputerowej. **Materiał i metody:** Badanie objęło 92 skany tomografii komputerowej zatok przynosowych u dzieci, z zatokami szczękowymi oznaczonymi ręcznie przez ekspertów ludzkich. Opracowano trójwymiarową konwolucyjną sieć

neuronową do segmentacji zatok. Na podstawie wyników segmentacji obliczono objętość zatok oraz procentowy stopień ich zajęcia przez zmiany zapalne. **Wyniki:** Algorytm wykazuje wysoką jakość segmentacji, osiągając średnie wartości czułości, precyzji oraz współczynnika Dice na poziomie prawie 90%. Średniokwadratowy błąd oszacowania objętości zatok oraz stopnia ich zajęcia wynosi odpowiednio 0,4 cm^3 oraz 1,3 punktu procentowego. **Wnioski:** Zaproponowane podejście umożliwia szybką i dokładną ocenę objętości zatok szczękowych oraz stopnia ich zapalnego zajęcia w badaniach tomografii komputerowej u dzieci. Może ono stanowić cenne narzędzie wspomagające decyzje kliniczne w diagnostyce oraz monitorowaniu przewlekłych chorób zatok przynosowych w populacji pediatrycznej.

Słowa kluczowe: przewlekłe zapalenie zatok przynosowych u dzieci, zatoka szczękowa, analiza objętościowa, tomografia komputerowa, segmentacja obrazów medycznych, konwolucyjna sieć neuronowa, uczenie głębokie, sztuczna inteligencja

INTRODUCTION

Disorders of the paranasal sinuses represent a significant health concern in the paediatric population. Maxillary sinusitis is one of the most common forms of sinus disease in children and may occur in either an acute or chronic form[1]. Clinical symptoms are often nonspecific and vary depending on the age child's age[2]. The prevalence of chronic rhinosinusitis (CRS) in children is lower than in adults and is estimated at 2–4%. However, the associated impairment in quality of life is comparable[3]. In the paediatric population, CRS is a consequence of frequent upper respiratory tract infections, incomplete craniofacial development, immaturity of the immune system, coexisting adenoid hypertrophy, allergic disease, and other systemic conditions[4,5]. Untreated or inadequately treated sinusitis may lead to orbital and intracranial complications, as well as disturbances in the development of craniofacial structures[1]. Children are particularly predisposed to orbital complications[6].

Medical imaging plays a key role in the diagnosis of paranasal sinus disease. Computed tomography (CT) is considered the reference modality for the assessment of paranasal sinus anatomy and the extent of sinus involvement[1]. Compared with other imaging techniques, CT enables accurate evaluation of mucosal thickness and fluid accumulation, while also demonstrating high sensitivity for the detection of inflammatory changes[7]. In paediatric patients, however, interpretation of CT images requires consideration of dynamic developmental changes that affect sinus volume and morphology[5,8]. Assessment of paranasal sinus involvement on CT is an integral component of the diagnostic workup for chronic and recurrent sinus disease. It is also a critical factor in determining eligibility for surgical treatment in patients with CRS. Classical scoring systems, such as the Lund–Mackay scale, offer a framework for the standardised classification of CT findings[9]. However, they rely on simplified categorical assessment of the presence or absence of sinus involvement, without precise quantification of its extent. Likness et al. and Kuo et al. demonstrated that the Lund–Mackay scale frequently fails to reflect the actual degree of sinus opacification accurately[10,11]. Furthermore, they argued that quantitative estimation of the involved sinus volume correlates more strongly with clinical symptoms.

Quantitative volumetric analysis may significantly improve diagnostic precision and facilitate objective monitoring of disease progression and treatment response. However, even computer-assisted volumetric measurements based on conventional algorithms, such as region growing, remain prohibitively time-consuming, hindering their use in clinical practice. This limitation may be addressed through the application of machine-learning methods, particularly neural networks.

Advances in artificial intelligence have created novel opportunities for the automated analysis of medical images. Machine-learning algorithms are increasingly being integrated into paediatric radiology[12]. Lee et al. demonstrated that a convolutional neural network could reproduce Lund–Mackay sinus opacification scores with high agreement[13]. Their automated system exhibited robust reproducibility and reduced interobserver variability compared with manual assessment.

Sun et al. employed a neural network to delineate the osseous structures of the paranasal sinuses for surgical planning and neuronavigation[14]. Whangbo et al. utilised a multiclass segmentation approach to identify individual cavities of the ethmoid, frontal, maxillary, and sphenoid sinuses[15]. Humphries et al. trained a neural network to segment the paranasal sinuses as a single structure, thereby enabling estimation of their total volume[16]. By applying appropriate Hounsfield-unit thresholds, they were also able to quantify the proportion of mucosal opacification. More recently, Kuo and Liu developed a machine-learning model to segment each sinus cavity separately, computing both its volume and degree of inflammatory involvement[17]. This line of research was subsequently continued by Wang et al. and Kaygısız Yiğit et al.[18,19]

Although these studies demonstrated good agreement between model predictions and expert annotations, their models were developed and validated in adult or adolescent populations with fully developed sinus morphology. Additionally, they rely on large and computationally demanding neural architectures that require specialised hardware, which may limit their application in many clinical settings. To our knowledge, studies dedicated specifically to the paediatric population remain lacking, even though sinonasal disorders in children may lead to particularly severe and lifelong consequences.

 DOI: 10.15557/PiMR.2026.0012

In light of these considerations, the present study aimed to develop a machine-learning model for the automated, quantitative assessment of maxillary sinus involvement in children based on CT examinations of the paranasal sinuses. Our approach utilises a neural network to segment the maxillary sinuses from digitally reconstructed CT images. Subsequently, a simple geometric algorithm distinguishes the left and right sinus cavities. Finally, voxels corresponding to air and mucus are quantified independently within each cavity to determine the extent of sinus involvement. The neural network was trained on a dataset of CT scans manually annotated by human experts. The following sections describe the individual components of the system, the characteristics of the dataset, and the training procedure, followed by an evaluation of model performance.

MODEL

In the proposed approach, each examined CT scan of the paranasal sinuses is first downsampled to a voxel size of $1 \times 1 \times 1$ mm^3. This reduced resolution still allows for reliable estimation of sinus volume and involvement while enabling the model to process images of any higher resolution, which encompasses virtually all modern CT scans. The resulting reduction in voxel count also allows the neural network to remain very compact.

The downsampled 3D image is used directly as input to the model. The network comprises only six convolutional layers and contains 424,993 parameters. The input image is processed in patches of $44 \times 44 \times 44$ voxels (equivalent to $44 \times 44 \times 44$ mm^3), which is sufficient to capture a substantial portion of even the largest maxillary sinuses observed in children.

The network's sole task is segmentation of the maxillary sinuses, without distinguishing between the left and right sides. Specifically, it assigns each input voxel a probability of belonging to the sinuses. Voxels located entirely outside or inside the sinuses are assigned values of 0 and 1, respectively, while voxels at the sinus boundaries receive intermediate values. This approach is analogous to anti-aliasing in digital imaging, and provides a smooth representation of sinus borders. A simple geometric algorithm is then employed to distinguish the two maxillary cavities, facilitating separate computation of their volume and involvement for the left and right sides.

The number of voxels identified within each cavity determines the sinus volume. The degree of involvement is estimated by quantifying voxels filled with air and mucus. Fig. 1 depicts a representative histogram of CT attenuation values across sinus voxels. Two distinct peaks are observed around 0 HU and −1000 HU, corresponding to mucus and air, respectively. However, a flat background is also present due to imperfections in digital image reconstruction and the presence of intermediate values at sinus boundaries. This makes it difficult or even impossible to define a sharp HU threshold separating air from mucus.

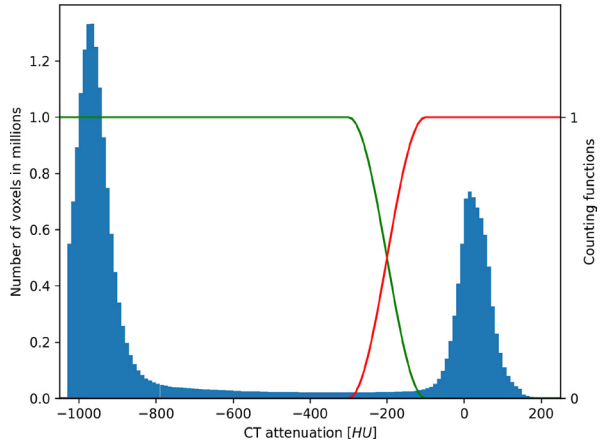

Fig. 1. Histogram of HU values within the maxillary sinuses, summed across all CT scans included in the present study. The green and red curves represent the functions used to estimate the free and involved volumes, respectively

To address this issue, two weights are assigned to each sinus voxel based on its CT attenuation value, following the two functions shown in Fig. 1. The red and green curves correspond to mucus and air, respectively. Voxels with attenuation below −300 HU are considered fully free, whereas those above −100 HU are considered fully involved. These thresholds were determined empirically by overlaying the weight colours on the CT images and confirming that free and involved regions appear uniformly green and red, respectively, with intermediate colours only at the boundaries. The transition between the two curves in Fig. 1 follows a half-wave sinusoid, representing a smooth threshold between free and involved HU values. This also guarantees that the two functions always sum to one. The free and involved volumes are then obtained by summing the corresponding weights across all voxels within each cavity.

DATASET

The neural network described in the previous section must be trained on a dedicated dataset. The dataset was constructed from the medical records of paediatric patients hospitalised in the Department of Paediatrics, Paediatric Nephrology and Allergology at the Military Institute of Medicine – National Research Institute in Warsaw, Poland, between 1 January 2020 and 31 December 2024. The dataset comprises CT scans of the paranasal sinuses obtained in children aged 0–18 years diagnosed with CRS based on CT assessment, physical examination, and medical history. Patients with acute rhinosinusitis or incomplete medical records were excluded from the analysis.

Three-dimensional CT images were acquired using a GE Medical Systems scanner with a spiral technique at 120 kV and reconstructed with the sharpening Bone or Bone Plus filter. All scans have comparable voxel dimensions of approximately $0.3 \times 0.3 \times 0.6$ mm^3 and a matrix size of 512×512 voxels in the transverse plane, with several

DOI: 10.15557/PiMR.2026.0012

hundred voxels along the body axis. A total of 92 three-dimensional images were manually segmented by five human experts who labelled each voxel as either belonging to the maxillary sinuses or not. This time-consuming process was facilitated using the open-access 3D Slicer software for medical image analysis (www.slicer.org)[20].

Human segmentations accurately capture the overall shape of the sinus cavities but are often imprecise at the level of individual voxels, particularly near septa. To address this, simple image-processing operations are applied to the human label maps. These operations smooth the segmentation boundaries and separate them from the internal sinus walls, preventing wall tissues from being incorrectly classified as mucus. They also convert the original binary labels into floating-point fuzzy labels, which can be directly compared with the probabilities predicted by the neural network.

The 92 scans comprise 184 maxillary sinuses, evenly divided between left and right sides. Fig. 2 presents a scatter plot of all sinuses in the volume-involvement plane. Sinus volumes in the dataset range from less than 2 cm^3 to more than 25 cm^3, consistent with the patient age range of 0–18 years. All degrees of involvement are represented, from completely aerated to fully involved. The data may suggest that smaller sinuses tend to exhibit a higher degree of involvement, a finding consistent with established medical knowledge.

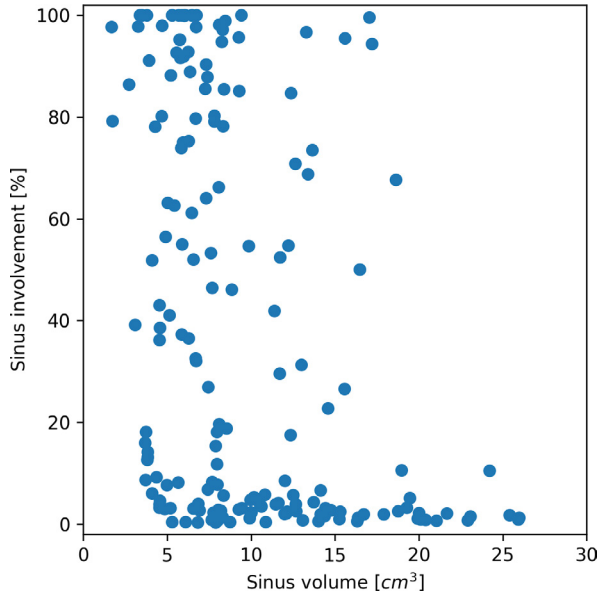

Fig. 2. Sinus involvement plotted against cavity volume for all 184 maxillary sinus cavities across the 92 CT scans in the dataset created for the present study

TRAINING

The goal of training the neural network is to reproduce the human segmentations when provided with their corresponding CT images. A properly designed network trained on sufficiently large and diverse data can then generalise this knowledge to segment new scans, previously unseen in the training dataset. The training workflow proceeds as follows.

First, the human label maps are downsampled to a voxel size of 1 × 1 × 1 mm^3 along with their corresponding CT images. Second, both images and segmentations are randomly rotated and translated as a form of data augmentation. This technique is commonly used in machine learning to make the training data more diverse and helps the network learn to process images at different positions and orientations[12].

The augmented images are then passed to the neural network, which produces its own fuzzy segmentations or label maps. Their deviation from the human maps is quantified using a loss function. This loss is minimised with respect to the 424,993 network parameters using the popular Adam optimisation algorithm[21]. As the loss or deviation approaches zero, the segmentations yielded by the network become increasingly similar to the true human annotations. A total of nearly one million minimisation steps is required to train the model, which takes approximately five days on a PC equipped with a gaming-class 12 GB graphics card. The card serves as a hardware accelerator for complex mathematical operations. Training was performed using a cluster of 16 more advanced graphics cards available at the Military Institute of Medicine – National Research Institute.

EVALUATION

To assess the final performance of the trained model, the entire dataset is usually split into validation and training sets in the conventional 1:4 ratio. Loss is minimised uniquely on the training set, after which performance metrics are estimated for the validation set. In this way, the model is evaluated only on previously unseen scans, reflecting the real clinical setup.

The validation set should include scans of varied sinus volume and degrees of involvement to be representative for the entire dataset. Additionally, some choices may inadvertently underestimate or overestimate true performance, so that several validation sets should be considered for a reliable assessment. Accordingly, a widely used testing procedure, known as Monte Carlo cross-validation, was applied[22].

Using the K-Means algorithm, the 92 scans were clustered into groups with similar sinus volume and congestion[23]. From each group, one scan was randomly chosen for validation, with the remaining scans included in the training set. Ten independent pairs of training and validation sets were randomly selected in this manner. For each pair, full loss minimisation was performed on the training set, followed by evaluation of performance metrics on the validation set. The arithmetic means and standard deviations across these ten runs are reported below as the final values and uncertainties of the performance metrics.

For sinus segmentation alone, the model achieves a true-positive rate (recall, sensitivity) of 89.0 ± 0.5%, a positive

 DOI: 10.15557/PiMR.2026.0012

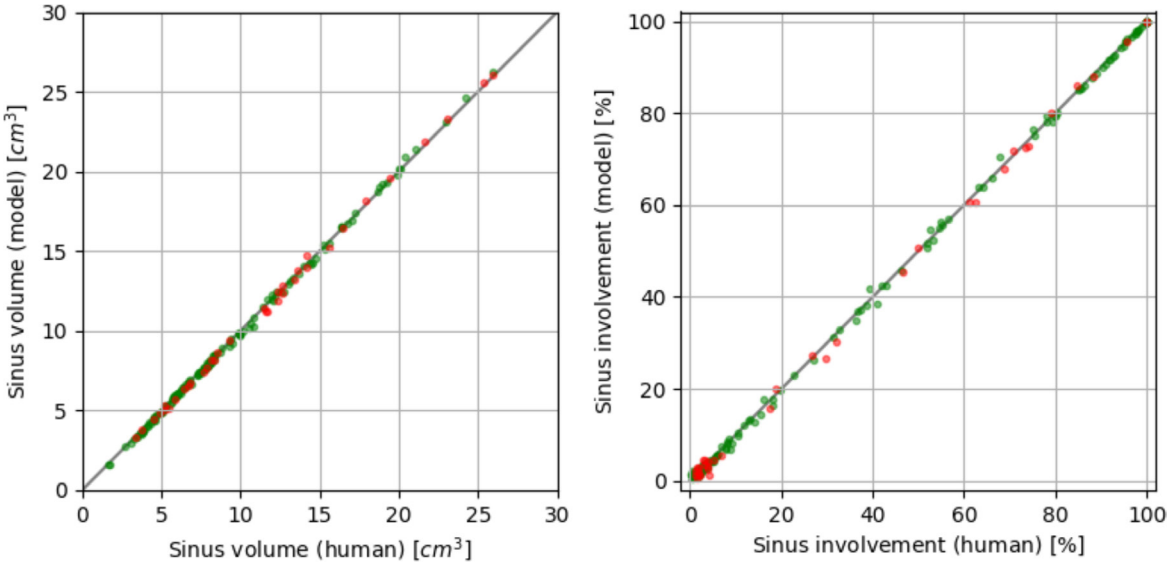

Fig. 3. Maxillary sinus volume (left) and involvement (right) estimated by the machine-learning model versus reference values computed from human expert segmentations. Red and green points correspond to the validation and training sets, respectively

predictive value (precision) of 90.0 ± 0.3%, and an F1 (Dice) score of 89.5 ± 0.3%[24]. For the estimation of sinus volume and involvement, the root-mean-square errors are 0.4 ± 0.2 cm³ and 1.3 ± 0.3 percentage points, respectively. To illustrate the achieved accuracy, Fig. 3 shows the sinus volume and involvement predicted by the model plotted against the reference values obtained from human segmentations. The data points align closely along the straight line representing perfect agreement for both the training and validation sets.

SOFTWARE

The trained model has been integrated into a user-friendly graphical application, illustrated in Fig. 4. The application reads a three-dimensional CT image from a DICOM (Digital Imaging and Communications in Medicine) file and displays its two-dimensional cross-sections, with free and involved regions highlighted in green and red, respectively. It also reports the volume and percentage of involvement for the left and right maxillary sinuses. The programme runs smoothly even on mid-range laptops, completing segmentation and prediction in approximately 10 seconds.

DISCUSSION

As noted in the Introduction, recent literature describes extensive work on paranasal sinus segmentation from CT scans[12–19]. Although these studies also employ neural networks, they focus on adults or adolescents. Automatic examination of sinuses in children is inherently more complex due to less pronounced anatomical structures and their dynamic changes with age. At the same time, children are more susceptible to sinus pathologies, such as CRS, and untreated or inappropriately managed sinonasal abnormalities may lead to severe, lifelong complications. In this context, the present work is a pioneering effort to develop machine-learning models specifically tailored to the paediatric population.

A neural network is introduced for automatic segmentation of the maxillary sinuses in paediatric CT examinations. The resulting segmentations are subsequently used to estimate sinus volume and the degree of mucosal involvement. The system achieves a volumetric accuracy of 0.4 ± 0.2 cm³ and a precision of 1.3 ± 0.3 percentage points for involvement estimation. These values are significantly more precise than a human inspection of a CT scan could ever provide.

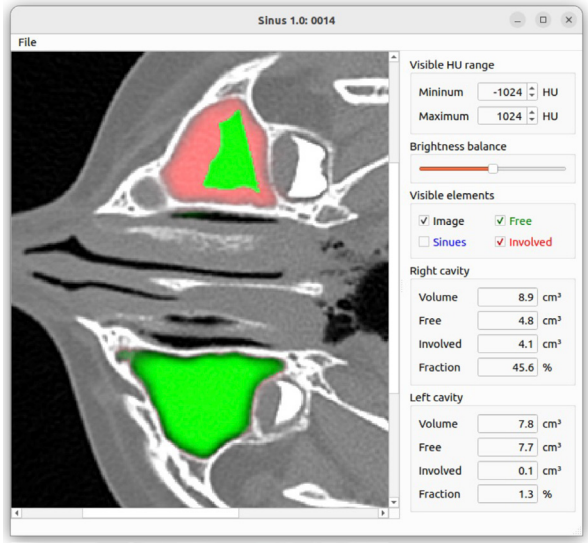

Fig. 4. Graphical user interface of the proposed model. Free and involved areas are highlighted in green and red, respectively. Total, free, and involved volumes, as well as the fraction of involvement, are displayed separately for each side

DOI: 10.15557/PiMR.2026.0012

Furthermore, the model maintains the same fidelity that is achieved by state-of-the-art neural architectures tested so far in adult populations, despite the difficulties associated with immature sinus anatomy.

An important methodological strength of the present study is the use of fuzzy labels for both human annotations and model outputs[25]. In contrast to the conventional binary labelling employed by most previous studies in this field, this approach more faithfully captures the inherent ambiguity of anatomical boundaries and effectively addresses the partial-volume effect introduced by the finite resolution of CT imaging. For instance, if a voxel is located at the sinus boundary, a fractional label can correctly reflect the fact that it is partially occupied by air and partially by mucosal tissue.

A distinctive feature of this system is its simplicity. The neural network contains only 424,993 parameters, which is very modest compared with most medical imaging solutions that include from 1.5 million to 1.5 billion parameters. This allows the model to run smoothly even on mid-range laptops without dedicated high-performance graphics hardware. On such devices, the software completes segmentation and prediction in about 10 seconds. This efficiency facilitates deployment across diverse clinical settings, from hospital departments to single-physician outpatient practices. The resulting segmentation maps, with aerated and involved regions marked in colour, are displayed as overlays on CT images, allowing immediate visual verification by the clinician.

From a clinical perspective, the presented tool provides a rapid, accessible, reproducible, quantitative, and precise assessment of the maxillary sinus volume and mucosal involvement. It has the potential to reduce inter-observer variability and thus enhance the standardisation of CT evaluations in children with CRS. The tool may be particularly valuable for objective longitudinal monitoring of disease progression and treatment response.

One constraint of the current study is the focus on the maxillary sinuses alone. Another limitation is that all scans were acquired using a single CT scanner. Consequently, the generalisability of a machine-learning model trained on this dataset to scans acquired using other systems remains uncertain. Nevertheless, the dataset is unique in international literature. To the best of our knowledge, only the NasalSeg and CT-SCOPE datasets are partially comparable[26,27]. However, they focus primarily on adult populations, provide lower spatial resolution, or target segmentation of bony structures rather than sinus volume.

Given these limitations, the overall success of the present study supports further development and refinement. More diverse training data should be collected in the future. The ethmoid, frontal, and sphenoid sinuses can be annotated by human experts to enable the system to segment all paranasal sinuses. Other structures, such as the ostiomeatal complex or nasolacrimal ducts, can be also considered. CT scans from patients with acute rhinosinusitis could be included as well, extending the system's applications across different inflammatory phenotypes. Finally, experts may annotate various lesions, such as retention cysts, polyps, and osteitis, as well as anatomical variants including concha bullosa and Haller or Onodi cells, enabling the model to detect them.

Apart from these relatively straightforward improvements, more advanced extensions of the current framework can be envisaged. One involves training the model to estimate the anatomical age of the sinuses based on morphological development and pneumatisation patterns. By comparing the result with the patient's chronological age, clinicians could assess, to a certain extent, whether the paranasal sinuses are developing appropriately or exhibit signs of developmental delay, including hypoplasia.

Preliminary experiments indicate that the model, when integrated with complementary algorithms, can quantitatively estimate the patency of the entire drainage and ventilation pathway extending from the sinus ostia through the ostiomeatal complex to the nasal cavity. Accurate assessment of these narrow, convoluted channels is often challenging for radiologists, particularly in cases of complex or variant anatomy. Quantifying the patency of the outflow and aeration tracts could provide a clinical explanation for symptomatic patients whose sinus cavities appear clear on CT.

CONCLUSIONS

The proposed machine-learning algorithm enables automated and precise assessment of maxillary sinus volume and inflammatory involvement in children with CRS. The method demonstrates high agreement with expert segmentation, operates on standard computer hardware, and provides immediate, visually verifiable results. This approach represents a promising step toward objective, reproducible, and standardised imaging evaluation of paediatric CRS and may serve as a foundation for broader, multi-sinus automated assessment in the future.

Ethics approval and informed consent statement

All data were obtained from the hospital registry of the Military Institute of Medicine – National Research Institute in Warsaw, Poland, and were fully anonymised prior to analysis. The study protocol was approved by the Institute's Bioethics Committee (No. 7/26). Due to the retrospective design and the use of anonymous records, the requirement for informed consent was waived.

Author contribution

Original concept of study: AT, AZ, BK. Collection, recording and/or compilation of data: AZ, JG, PO. Analysis and interpretation of data: AT, AZ, JG, NG, PO. Software and Methodology: JG, PO. Writing of manuscript: AT, AZ, JG, NG, PO. Critical review of manuscript: AT, BK, PO.

Acknowledgments

This publication was developed within the project "Establishment of the Digital Medicine Centre of the Military Institute of Medicine –

National Research Institute and the University of Warsaw", funded by the state budget through the Medical Research Agency under the call "Development of Regional Digital Medicine Centres". We sincerely thank the Department of Teleinformatics and the Regional Digital Medicine Centre at the Military Institute of Medicine for providing access to the computing cluster and preparing the CT image database.

References

1. Fokkens WJ, Lund VJ, Hopkins C et al.: European position paper on rhinosinusitis and nasal polyps 2020. Rhinology 2020; 58 (Suppl S29): 1–464.
2. Kasprzyk A, Niedzielski A: Przewlekłe zapalenie zatok przynosowych u dzieci – przegląd aktualnego piśmiennictwa. Now Audiofonol 2020; 9: 11–15.
3. Arcimowicz M, Niemczyk K: EPOS2020: co nowego dla lekarza praktyka? Pol Otorhino Rev 2020; 9: 7–17.
4. Hamilos DL: Pediatric chronic rhinosinusitis. Am J Rhinol Allergy 2015; 29: 414–420.
5. Brietzke SE, Shin JJ, Choi S et al.: Clinical consensus statement: pediatric chronic rhinosinusitis. Otolaryngol Head Neck Surg 2014; 151: 542–553.
6. Capra G, Liming B, Boseley ME et al.: Trends in orbital complications of pediatric rhinosinusitis in the United States. JAMA Otolaryngol Head Neck Surg 2015; 141: 12–17.
7. Bhattacharyya N, Jones DT, Hill M et al.: The diagnostic accuracy of computed tomography in pediatric chronic rhinosinusitis. Arch Otolaryngol Head Neck Surg 2004; 130: 1029–1032.
8. Chandy Z, Ference E, Lee JT: Clinical guidelines on chronic rhinosinusitis in children. Curr Allergy Asthma Rep 2019; 19: 14.
9. Lund VJ, Mackay IS: Staging in rhinosinusitis. Rhinology 1993; 31: 183–184.
10. Likness MM, Pallanch JF, Sherris DA et al.: Computed tomography scans as an objective measure of disease severity in chronic rhinosinusitis. Otolaryngol Head Neck Surg 2014; 150: 305–311.
11. Kuo CFJ, Liao YS, Barman J et al.: Semi-supervised deep learning semantic segmentation for 3D volumetric computed tomographic scoring of chronic rhinosinusitis: clinical correlations and comparison with Lund-Mackay scoring. Tomography 2022; 8: 718–729.
12. Litjens G, Kooi T, Bejnordi BE et al.: A survey on deep learning in medical image analysis. Med Image Anal 2017; 42: 60–88.
13. Lee DJ, Hamghalam M, Wang L et al.: The use of a convolutional neural network to automate radiologic scoring of computed tomography of paranasal sinuses. Biomed Eng Online 2025; 24: 49.
14. Sun Y, Guerrero-López A, Arias-Londoño JD et al.: Automatic semantic segmentation of the osseous structures of the paranasal sinuses. Comput Med Imaging Graph 2025; 123: 102541.
15. Whangbo J, Lee J, Kim YJ et al.: Deep learning-based multi-class segmentation of the paranasal sinuses of sinusitis patients based on computed tomographic images. Sensors (Basel) 2024; 24: 1933.
16. Humphries SM, Centeno JP, Notary AM et al.: Volumetric assessment of paranasal sinus opacification on computed tomography can be automated using a convolutional neural network. Int Forum Allergy Rhinol 2020; 10: 1218–1225.
17. Kuo J, Liu SC: Fully automatic segmentation, identification and preoperative planning for nasal surgery of sinuses using semi-supervised learning and volumetric reconstruction. Mathematics 2022; 10: 1189.
18. Wang Y, Zhang X, Du W et al.: Deep learning-based fully automatic segmentation of the paranasal sinuses in chronic rhinosinusitis patients using computed tomographic images. IEEE Access 2025; 13: 16444–16454.
19. Kaygısız Yiğit M, Pınarbaşı A, Etöz M et al.: Artificial intelligence-based fully automatic 3D paranasal sinus segmentation. Dentomaxillofac Radiol 2026; 55: 61–72.
20. Fedorov A, Beichel R, Kalpathy-Cramer J et. al.: 3D Slicer as an image computing platform for the Quantitative Imaging Network. Magn Reson Imaging 2012; 30: 1323–1341.
21. Kingma DP, Ba JL: Adam: a method for stochastic optimization. arXiv 2017; 1412.6980.
22. Xu QS, Liang YZ, Du YP: Monte Carlo cross-validation for selecting a model and estimating the prediction error in multivariate calibration. J Chemom 2004; 18: 112–120.
23. MacQueen J: Some methods for classification and analysis of multivariate observations. Proceedings of the 5th Berkeley Symposium on Mathematical Statistics and Probability 1967; 5.1: 281–297.
24. Dice LR: Measures of the amount of ecologic association between species. Ecology 1945; 26: 297–302.
25. Taha AA, Hanbury A: Metrics for evaluating 3D medical image segmentation: analysis, selection, and tool. BMC Med Imaging 2015; 15: 29.
26. Zhang Y, Wang J, Pan T et al.: NasalSeg: a dataset for automatic segmentation of nasal cavity and paranasal sinuses from 3D CT images. Sci Data 2024; 11: 1329.
27. Sun Y, Guerrero-López A, Arias-Londoño JD et al.: CT-SCOPE: annotated dataset of CT SCans for the automatic semantic segmentation of the Osseous structures of the Paranasal sinusEs. Data Brief 2025; 62: 111962.